Journal of Fusion Energy, Vol. 26, Nos. 1/2, June 2007 (© 2006)
DOI: 10.1007/s10894-006-9041-6

On the Physics of Improved Confinement During Pulsed Poloidal Current Drive in MST Reversed-Field Pinch

V. A. Svidzinski[1,*] and S. C. Prager[1]

Reduction of core-resonant magnetic fluctuations and improved confinement in the Madison Symmetric Torus reversed-field pinch (MST RFP) have been routinely achieved by applying the surface poloidal electric field. The created inductive poloidal electric field drives current in plasma which leads to the improved confinement. To study the effect we developed a relatively simple 1-D model in cylindrical geometry which assumes poloidal and axial symmetry during the drive. We use resistive magnetohydrodynamics model with realistic plasma parameters and assume that there is a vacuum gap between plasma boundary and conducting wall of the vessel. Evolution of plasma density is taken into account and plasma boundary moves self-consistently with momentum equation. We start from an initial unstable equilibrium and examine stability of plasma configuration at intermediate moments of time during the drive. For this we calculate the growth rates of unstable eigenmodes in the plasma. Our results show that the modifications to the plasma current profile during the drive are stabilizing. The initial stabilization is due to the direct modification of the current profile near the edge. It enhances later in time due to the flattening of λ profile in the core region as plasma and magnetic field compress inward during the drive.

KEY WORDS: Pulsed poloidal current drive; reversed field pinch; fluctuations.

INTRODUCTION

The reversed-field pinch (RFP) is a toroidal magnetically confined plasma. Toroidal magnetic field in RFP reverses direction in the plasma edge relative to its direction in the core. RFP plasmas exhibit large-amplitude, internally resonant magnetic fluctuations which allow rapid radial transport of particles and energy. These fluctuations are driven primarily by the gradient in the current density profile. The current in the RFP is driven both by the applied toroidal electric field and the self-generated dynamo electric field. The dynamo electric field arises from the correlated product of velocity and magnetic fluctuations. In standard RFP discharges, the applied toroidal electric field constitutes antiparallel current drive in the region outside the toroidal magnetic field reversal radius. The parallel current in this region in the Madison Symmetric Torus (MST) (Ref.[1]) has been shown to be driven by the mygnetohydrodynamic (MHD) dynamo [2–4].

An auxiliary edge current drive is applied to RFP plasmas with the goal of replacing the dynamo-driven current and modifying the parallel current profile to reduce current-driven instability. In the current-drive technique, called pulsed poloidal current drive (PPCD), a poloidal (parallel) electric field is induced by transiently increasing the reversed toroidal magnetic flux in the edge [5–9]. In the MST RFP this auxiliary current drive reduces magnetic and electrostatic fluctuations everywhere in the plasma and significantly improves plasma confinement [10].

[1] University of Wisconsin-Madison, Madison, WI, 53706, USA.
* To whom correspondence should be address. E-mail: vsvidzinski@wisc.edu.

MODEL DESCRIPTION

The 3-D resistive MHD modeling in cylindrical geometry has been used by several groups to study the effect. Due to limitations in computing power, such models are using smaller Lundquist numbers and assume that plasma density is constant during the drive. With these limitations and the ambiguity of the results the exact mechanism of fluctuation reduction is not evident from such modeling.

We developed a relatively simple 1-D model in cylindrical geometry which assumes poloidal and axial symmetry during the drive. The model uses resistive MHD equations and allows to make estimates based on realistic plasma parameters. We assume that there is a vacuum gap between plasma boundary and conducting wall of the vessel. Plasma is compressible and its boundary moves self-consistently with momentum equation. The vacuum gap with the free plasma boundary is used in the model in order to avoid difficulties in simulations arising when plasma density depletes near the edge due to the applied electric field.

The model details are as follows. Plasma is in a cylindrical vessel with radius a. Plasma can move only in radial direction, its radius is $r_p < a$. The vacuum gap is in the region $r_p < r < a$. Plasma density is finite for $r \le r_p$ and it is zero in the gap. Axially and azimuthally symmetric electric field $E_\theta(t)$ is specified at $r = a$. It has only poloidal component. This field corresponds to the inductive part of the electric field driven during PPCD.

In the experiment the voltage is applied to a cut in the shell which extends horizontally around the torus. This voltage is compensated by the inductive electric field (assuming high conductivity of the aluminum shell) created by the change of toroidal magnetic flux. The inductive electric field on the shell's surface is compensated by the potential electric field created by electrical charges in the shell localized near the cut, such that the resultant poloidal electric field on the shell's surface is zero. These charges compensate the poloidal electric field on the shell's surface but magnify it significantly in front of the cut. The electric field inside the torus is a superposition of the inductive electric field and the potential field created by the charges near the cut. The potential electric field does not drive current in the plasma and it is compensated by the induced charges near the plasma surface. Thus in our model we consider only inductive part of the electric field E_θ and impose it at $r = a$.

$E_\theta(t)$ starts from zero at $t = 0$ and is turned on to a constant value (in time) during short time interval (much smaller than the considered time of PPCD). At $t = 0$ plasma is in some force free cylindrical equilibrium. At $t > 0$ plasma motion is described by the resistive MHD equations in the limit of zero pressure (which is the only approximation beyond symmetry) where $S = \tau_R/\tau_A$ is the Lundquist number and the standard normalization is used (see, e.g., Ref.[11]). Electric and magnetic fields in the vacuum gap are evolved according to Maxwell's equations in the limit of slow time dependence. The boundary conditions across plasma–vacuum boundary are the continuity of tangential components of electric and magnetic fields (assumption of zero surface currents).

$$
\begin{aligned}
\frac{\partial \rho}{\partial t} &= -\frac{1}{r}\frac{\partial}{\partial r}(r\rho v_r),\\
\frac{\partial v_r}{\partial t} &= -v_r\frac{\partial v_r}{\partial r} - \frac{1}{\rho}\left[B_z\frac{\partial B_z}{\partial r} + \frac{1}{r}\frac{\partial}{\partial r}(rB_\theta)B_\theta\right],\\
\frac{\partial B_\theta}{\partial t} &= -\frac{\partial}{\partial r}(v_r B_\theta) + \frac{1}{S}\left[\left(\frac{\eta}{r} + \frac{\partial \eta}{\partial r}\right)\frac{\partial B_\theta}{\partial r} + \eta\frac{\partial^2 B_\theta}{\partial r^2} + \frac{1}{r}\left(\frac{\partial \eta}{\partial r} - \frac{\eta}{r}\right)B_\theta\right],\\
\frac{\partial B_z}{\partial t} &= -\frac{1}{r}\frac{\partial}{\partial r}(rv_r B_z) + \frac{1}{S}\left[\left(\frac{\eta}{r} + \frac{\partial \eta}{\partial r}\right)\frac{\partial B_z}{\partial r} + \eta\frac{\partial^2 B_z}{\partial r^2}\right],
\end{aligned}
$$

Total time of the electric field drive is taken to be $t_0 = 7$ ms. Initial plasma resistivity profile is $\eta = \eta_0[1 + 4(r/r_p)^6]$. We specify its time evolution as $d\eta/dt = 0$. Initial plasma density is constant with radius. Current profiles near the edge during the drive are very sensitive to the value of resistivity there. Calculations with different resistivity profiles, however, lead to similar conclusions about stabilization of

core resonant modes (the modes resonant in the region where safety factor q is positive). Thus the results obtained for the above resistivity profile should be considered as typical ones in the mentioned sense.

During time evolution intermediate plasma equilibria are almost force free. Thus a scaling with τ_R is suitable in our case. Namely, the result does not change for transformation $B = \tilde{B}$, $E = \tilde{E}/\alpha$, $v = \tilde{v}/\alpha$, $t = \tilde{t}\alpha$, $S = \tilde{S}\alpha$, $J = \tilde{J}$, $\rho = \tilde{\rho}$ as long as time scale is large relative to τ_A. This scaling is confirmed numerically. The scaling is applied for faster calculations and for obtaining the result with realistic S.

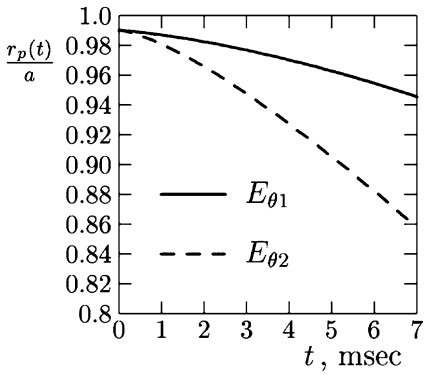

Fig. 1. Radial location of the plasma boundary vs. time for two different amplitudes of the applied electric field.

RESULTS

We consider plasma parameters typical to standard RFP discharges in MST, $B_0 = 1.5$ kG, $n_0 = 10^{13}$ cm^{-3}, we take $\tau_A = 0.7\mu$s. The results of calculation correspond to $S = 10^6$ and two values of applied electric field are considered, $E_{\theta\,1} = 0.3$ V/m, $E_{\theta\,2} = 0.6$ V/m. These electric fields are comparable with the ones driven in the experiment and the magnetic field reversal at the end of the drive calculated with these fields is comparable to the experimentally observed one as well.

Magnetic field in the RFP is nearly poloidal at the edge. Because of high plasma conductivity along magnetic field, the driven inductive electric field is shielded by plasma currents. During the drive there is a repulsive force between the image currents in plasma and current driven in the conducting shell by the applied voltage. The image current is opposite to the one in the shell and it is trying to shield the magnetic field created by current in the shell. The resultant force is pushing plasma inward and drags with it the equilibrium magnetic field embedded in the plasma. This leads to compression (pinching) of magnetic field, plasma current and density toward the core region.

We take $r_p/a = 0.99$ at $t = 0$. Several initial equilibria were examined. We present here one case, the results for other equilibria are similar to the results reported here. The initial unstable force free equilibrium is described by $\lambda(r) = 2\Theta_0[1 - (r/r_p)^{\alpha_0}]$ with $\alpha_0 = 2.75$ and $P_0 = 1.75$, where $\lambda = (J \cdot B)/B^2$.

Figure 1 shows radial location of the plasma boundary versus time for the two different applied fields $E_{\theta 1}$ and $E_{\theta 2}$. Plasma boundary moves significantly inward during the drive, the displacement is larger for stronger electric field. This corresponds to plasma density depletion near the wall of the vessel. Reduction of plasma density in the vicinity of the wall is observed in the experiment and by itself can improve the confinement because of better thermal isolation of the plasma from the wall. Inward displacement of the plasma boundary is sensitive to the value of resistivity near the plasma edge. The

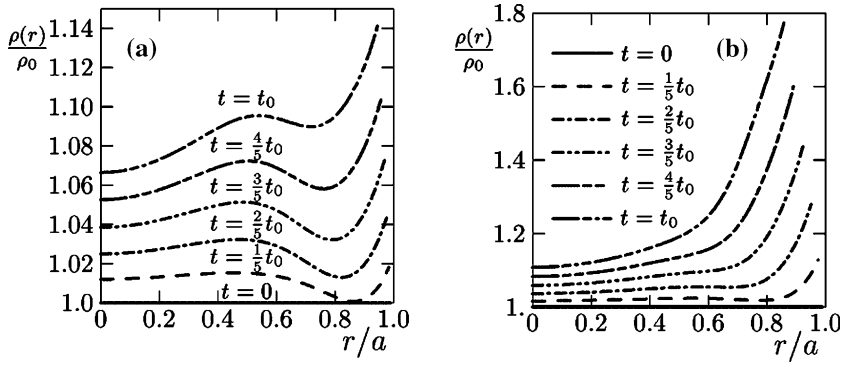

Fig. 2. Plasma density profiles at different moments of time. (a) $E_\theta = 0.3$ V/m; (b) $E_\theta = 0.6$ V/m.

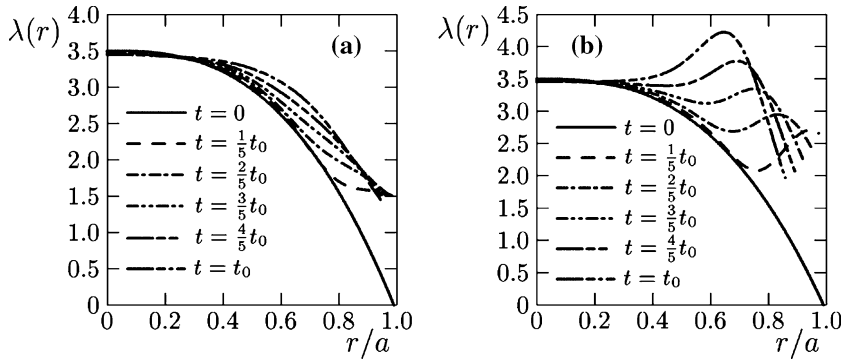

Fig. 3. λ profiles at different moments of time. (a) $E_\theta = 0.3$ V/m; (b) $E_\theta = 0.6$ V/m.

more resistive plasma edge the smaller the displacement. The inward displacement of the bulk plasma and the resulting compression of plasma density and magnetic field away from the edge are not sensitive to the edge resistivity profile. They depend on the core plasma resistivity (Lundquist number) which is a well defined parameter. Plasma boundary modeling, however, is important for the edge resonant (modes resonant where $q < 0$) and external modes.Such modes become unstable as the plasma boundary moves inward which is also observed in the experiment near the end of PPCD. Accurate modeling of the plasma boundary is beyond the scope of our analysis. Thus we consider only core resonant modes (resonant in the region with $q > 0$) in our study.

Figure 2 shows plasma density profiles at different moments of time for the two amplitudes of E_θ. Density in the central part increases noticeably while density modification near the edge is stronger. The density profiles near the edge are sensitive to the edge plasma resistivity. As expected the density perturbation is stronger for larger E_θ. Density peak at the plasma boundary is the result of sharp plasma–vacuum transition and of the limit of zero pressure in our model. Some increase of the core plasma density is in line with the experimentally observed one.

Profiles of $\lambda = (J \cdot B)/B^2$ at different moments of time for the two E_θ are shown in Figure 3. Edge current profile changes rapidly and significantly during the drive. The effect is stronger in stronger electric field. Plasma current perturbation reaches central part on Alfvénic time scale. The λ profile there changes slowly and the changes become noticeable later in time. The changes lead to flattening of the λ profile in the core.

In our model there is no maintained axial electric field such that all profiles decay slowly on resistive time scale without the drive. That is why in the above plots the λ profiles in the core are somewhat edged down later in time. In the limit of high S the profiles are staying approximately constant at $r = 0$ such that there is a simultaneous increase of current and magnetic field there.

To check on the importance of plasma compression (nonzero v_r) for the profile flattening we calculated λ profiles in the case when the condition $v_r(r) = 0$ is enforced artificially. This is equivalent to resistive diffusion of electric field in the plasma. In this case there are no changes in the λ profile beyond the region where the electric field can penetrate during the drive due to plasma resistivity (approximately one third of the plasma radius).

Profiles of magnetic field components at $t = 0$ ms and $t_0 = 7$ ms for the two amplitudes of E_θ are presented in Figure 4. For the better comparison the resistive decay is accounted for in the profiles corresponding to $t = 0$. The magnetic field and the plasma current increased in the core region by the end of the drive (this is more clearly seen in Figure 4b) while the value of λ is approximately unchanged at $r = 0$. The magnetic field reversal is magnified at the edge by the end of PPCD.

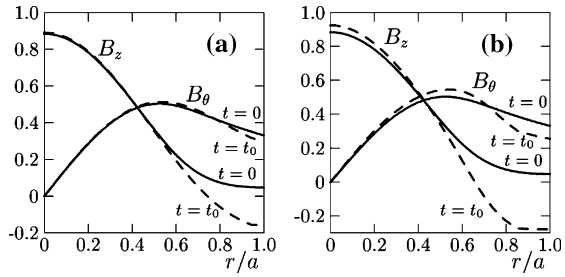

Fig. 4. Profiles of magnetic field components at different moments of time. (a) $E_\theta = 0.3$ V/m; (b) $E_\theta = 0.6$ V/m.

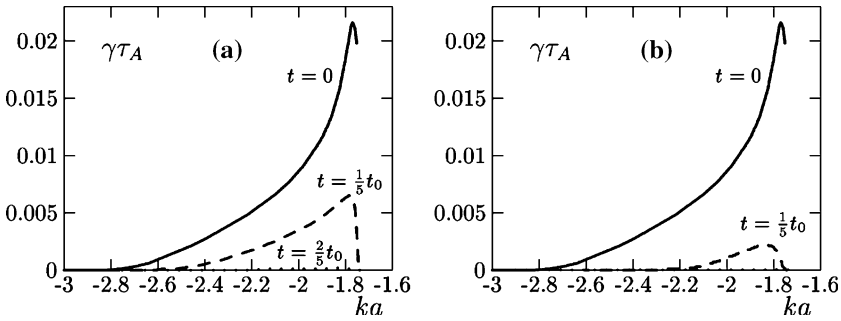

Fig. 5. Growth rate spectrum at different moments of time. (a) $E_\theta = 0.3$ V/m; (b) $E_\theta = 0.6$ V/m.

We examine the stability of force free equilibria with the λ profiles of Figure 3a,b. For this we developed a code which solves an eigenmodes problem for plasma described by resistive MHD equations in a cylinder with a vacuum gap between plasma and conducting wall. In the code the solution of Maxwell's equations in vacuum layer, combinations of modified Bessel functions, is matched with the numerical solution in the plasma. In the model plasma boundary can move freely and the excitation of a surface wave type structure near the plasma–vacuum boundary is observed.

We consider $m = 1$ modes, they are core resonant in RFP, and scan k continuously (m and k are poloidal and axial wave numbers). For a particular toroidal wave number n the resonant surface of a mode shifts during the drive and the mode stabilization can be because the resonance moves closer to the conducting wall. Thus the complete picture is better established with the continuous scan of k instead of scanning the discrete values of n. The growth rates are calculated for $S = 10^4$. While the analysis is not limited to a particular type of unstable modes, mainly tearing modes are excited.

Growth rates of unstable internally resonant modes versus ka for λ profiles at different moments of time during the drive are shown in Figure 5 for the two amplitudes of E_θ. The applied electric field transforms initially unstable current profile into a stable one on a relatively short time scale after the start of PPCD. Stable current profile is reached faster in stronger electric field. In the presented case in order to demonstrate the effect of stabilization we started from the initial equilibrium which is far from marginal stability. When the initial equilibrium is closer to marginal stability the stabilization of the current profile happens even faster.

The flattening of λ profile in the core at later times is a stabilizing factor. To understand what causes the stabilization at initial times the stability properties of the λ profiles of the types $\lambda = \lambda_0 + A \exp[-((r-r_p)/\triangle)^2]$ are examined. λ_0 is the profile at $t = 0$ and the parameters A and $\triangle$ are chosen such that the resultant profiles approximately fit the ones at different t. Such substitution ensures that the profile does not change in the core but approximately describes the edge current modification. We found that such profiles do stabilize the modes but to the lesser extent than the real profiles with the central current modification. They reduce the growth rates significantly but can not completely stabilize the modes.

SUMMARY

Thus we can conclude that during PPCD the initial plasma stabilization is due to the modification of the current profile near the edge and that this stabilization enhances later in time due to the flattening of λ profile in the core region.

REFERENCES

1. R. N. Dexter, D. W. Kerst, T. W. Lovell, S. C. Prager, and J. C. Sprott, *Fusion Technol.*, **19**, 131 (1991).
2. H. Ji, A. F. Almagri, S. C. Prager, and J. S. Sarff, *Phys. Rev. Lett.*, **73**, 668 (1994).
3. P. W. Fontana, Ph.D. thesis, University of Wisconsin-Madison, Madison, 1999.
4. P. W. Fontana, D. J. Den Hartog, G. Fiksel, and S. C. Prager, *Phys. Rev. Lett.*, **85**, 566 (2000).
5. J. S. Sarff, S. A. Hokin, H. Ji, S. C. Prager, and C. R. Sovinec, *Phys. Rev. Lett.*, **72**, 3670 (1994).
6. J. S. Sarff, N. E. Lanier, S. C. Prager, and M. R. Stoneking, *Phys. Rev. Lett.*, **78**, 62 (1997).
7. M. R. Stoneking, N. E. Lanier, S. C. Prager, J. S. Sarff, and D. Sinitsyn, *Phys. Plasmas*, **4**, 1632 (1997).
8. R. Bartiromo, P. Martin, S. Martini, T. Bolzonella, A. Canton, P. Innocente, L. Marrelli, A. Murari, and R. Pasqualotto, *Phys. Rev. Lett.*, **82**, 1462 (1999).

9. B. E. Chapman, T. M. Biewer, P. K. Chattopadhyay, C. S. Chiang, D. J. Craig, N. A. Crocker, D. J. Den Hartog, G. Fiksel, P. W. Fontana, S. C. Prager, and J. S. Sarff, *Phys. Plasmas*, **7**, 3491 (2000).
10. B. E. Chapman, A. F. Almagri, J. K. Anderson, T. M. Biewer, P. K. Chattopadhyay, C. S. Chiang, D. Craig, D. J. Den Hartog, G. Fiksel, C. B. Forest, A. K. Hansen, D. Holly, N. E. Lanier, R. O'Connell, S. C. Prager, J. C. Reardon, J. S. Sarff, and M. D. Wyman, *Phys. Plasmas*, **9**, 2061 (2002).
11. S. Ortolani and D. Schnack, *Magnetohydrodynamics of Plasma Relaxation* (World Scientific, 1993).